AD-A155 763 FINITE TEMPERATURE STABILIZATION OF THE GRADIENT DRIFT INSTABILITY IN BARIUM CLOUDS(U) NAVAL RESEARCH LAB WASHINGTON DC J F DRAKE ET AL. 21 MAY 85 NRL-MR-5566 1/1

UNCLASSIFIED F/G 20/9 NL

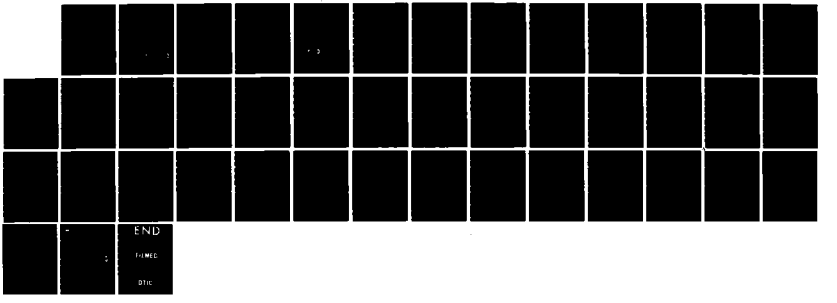

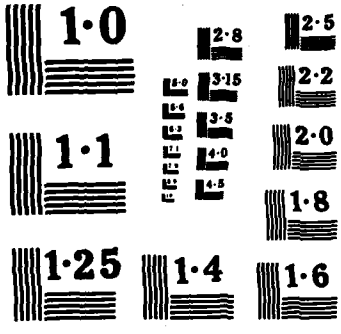

NATIONAL BUREAU OF STANDARDS
MICROCOPY RESOLUTION TEST CHART

NRL Memorandum Report 5566

Finite Temperature Stabilization of the Gradient Drift Instability in Barium Clouds

J. F. DRAKE

Science Applications International Corp.
McLean, VA 22102

J. D. HUBA AND S. T. ZALESAK

Geophysical and Plasma Dynamics Branch
Plasma Physics Division

May 21, 1985

This research was sponsored by the Defense Nuclear Agency under Subtask QIEQMXBB, work unit 00005 and work unit title "Plasma Structure Evolution."

NAVAL RESEARCH LABORATORY
Washington, D.C.

SECURITY CLASSIFICATION OF THIS PAGE

REPORT DOCUMENTATION PAGE

1a REPORT SECURITY CLASSIFICATION UNCLASSIFIED	1b. RESTRICTIVE MARKINGS
2a SECURITY CLASSIFICATION AUTHORITY	3 DISTRIBUTION / AVAILABILITY OF REPORT Approved for public release; distribution unlimited.
2b DECLASSIFICATION / DOWNGRADING SCHEDULE	
4 PERFORMING ORGANIZATION REPORT NUMBER(S) NRL Memorandum Report 5566	5 MONITORING ORGANIZATION REPORT NUMBER(S)
6a NAME OF PERFORMING ORGANIZATION Naval Research Laboratory 6b OFFICE SYMBOL (If applicable) Code 4780	7a NAME OF MONITORING ORGANIZATION
6c ADDRESS (City, State, and ZIP Code) Washington, DC 20375-5000	7b ADDRESS (City, State, and ZIP Code)
8a NAME OF FUNDING / SPONSORING ORGANIZATION Defense Nuclear Agency 8b OFFICE SYMBOL (If applicable) RAAE	9. PROCUREMENT INSTRUMENT IDENTIFICATION NUMBER
8c ADDRESS (City, State, and ZIP Code) Washington, DC 20305	10. SOURCE OF FUNDING NUMBERS PROGRAM ELEMENT NO. 62715H; PROJECT NO.; TASK NO.; WORK UNIT ACCESSION NO. DN580-072

11 TITLE (Include Security Classification)

Finite Temperature Stabilization of the Gradient Drift Instability in Barium Clouds

12 PERSONAL AUTHOR(S)

Drake, J.F.,* Huba, J.D. and Zalesak, S.T.

13a TYPE OF REPORT	13b TIME COVERED	14 DATE OF REPORT (Year, Month, Day)	15 PAGE COUNT
Interim	FROM 10/84 TO 10/85	1985 May 21	42

16 SUPPLEMENTARY NOTATION

*Science Applications International Corporation, McLean, VA 22102 (Continues)

17 COSATI CODES		
FIELD	GROUP	SUB-GROUP

18. SUBJECT TERMS (Continue on reverse if necessary and identify by block number)

Gradient drift instability
Ionospheric structure
Barium clouds

19 ABSTRACT (Continue on reverse if necessary and identify by block number)

We present a relatively simple analysis of the gradient drift instability in barium clouds which includes the effects of both finite temperature and finite parallel length. It is found that short wavelength modes are stabilized as the electrons redistribute parallel to the magnetic field and neutralize the charge imbalance set up by the instability. An analytical expression for the critical wavenumber for stabilization is given, as well as numerical results. We discuss the application of these results to the structuring of barium clouds.

20 DISTRIBUTION / AVAILABILITY OF ABSTRACT	21 ABSTRACT SECURITY CLASSIFICATION	
☒ UNCLASSIFIED/UNLIMITED ☐ SAME AS RPT ☐ DTIC USERS	UNCLASSIFIED	
22a NAME OF RESPONSIBLE INDIVIDUAL J. D. Huba	22b TELEPHONE (Include Area Code) (202) 767-3630	22c. OFFICE SYMBOL Code 4780

DD FORM 1473, 84 MAR 83 APR edition may be used until exhausted
All other editions are obsolete

SECURITY CLASSIFICATION OF THIS PAGE

16. SUPPLEMENTARY NOTATION (Continued)

This research was sponsored by the Defense Nuclear Agency under Subtask QIEQMXBB, work unit 00005 and work unit title "Plasma Structure Evolution."

CONTENTS

FINITE TEMPERATURE STABILIZATION OF THE GRADIENT DRIFT INSTABILITY IN BARIUM CLOUDS

I. INTRODUCTION

The study of the dynamic evolution of artificial plasma clouds (e.g., barium clouds) in the earth's ionosphere and magnetosphere has been an active area of research for more than two decades. The initial motivation for these active space experiments was to use the plasma cloud as a diagnostic to determine ambient plasma conditions (e.g., electric fields, neutral winds). ~~However,~~ it was ~~soon~~ discovered that the interaction of an artificial plasma cloud and the near-earth space plasma was very complex, and that plasma clouds undergo a complicated and dynamic evolution. One of the prominent features of cloud evolution in the ionosphere is the development of field-aligned striations on the cloud's steepened "backside". These striations have been attributed to the onset of the gradient drift instability ~~(Linson and Workman, 1970)~~. This instability can occur in a weakly collisional plasma which contains a density gradient and a neutral wind (or ambient electric field) ~~(Simon, 1963; Hoh, 1963)~~.

Keywords: Gradient drift instability and Ionospheric structure

A substantial amount of theoretical and computational research has been invested in understanding the linear and nonlinear development of the gradient drift instability and its relevance to plasma cloud structure (Volk and Haerendel, 1971; Perkins et al., 1973; Zabusky et al., 1973; Shiau and Simon, 1972; Perkins and Doles, 1975; Scannapieco et al., 1976; Chaturvedi and Ossakow, 1979; Keskinen et al., 1980; McDonald et al., 1980; McDonald et al., 1981; Huba et al., 1983). The bulk of analyses to date have neglected the effects of plasma dynamics parallel to the ambient magnetic field $\underset{\sim}{B}_0$ (i.e., considered perturbations only in the plane transverse to $\underset{\sim}{B}_0$) or have incorporated parallel effects in a crude way.

Manuscript approved February 22, 1985.

Francis and Perkins (1975), for example, assume that the ambient and perturbed potentials map uniformly along $\underset{\sim}{B}_0$ thereby connecting the cloud dynamics to that of the conducting background at different altitudes. In this model finite thermal effects have a stabilizing influence on short wavelength modes. However, several studies have been performed which attempt to include parallel dynamics self-consistently in the stability analysis (Goldman et al., 1976; Sperling and Glassman, 1984; Sperling et al., 1984). These studies incorporate the parallel length of the cloud along the ambient field into the stability analysis and have shown that parallel effects can play an important role in the development of the gradient drift instability as it relates to ionospheric plasma clouds.

In particular, Sperling et al. (1984) have recently shown that when the finite size of the cloud along $\underset{\sim}{B}_0$ is self-consistently incorporated in the linear stability analysis, the long wavelength modes tend to have much smaller growth rates than short wavelength modes. This reduction in growth due to finite cloud length occurs because the integrated Pedersen conductivity of the background plasma over the extent of the mode along the field becomes greater than the cloud. The distance the mode extends along the field is proportional to the perpendicular wavelength of the mode so that long wavelength modes are more strongly affected. However, this analysis neglected the effects of finite temperature. Sperling and Glassman (1984) included finite temperature in the analysis and found that short wavelength modes became propagating rather than purely growing modes. Moreover, for sufficiently short wavelengths there was some evidence that the modes were be completely stabilized. A drawback of this work though is that a relatively complex, second-order differential equation is solved numerically to obtain results. The underlying physics of the stabilization mechanism is therefore somewhat obscure and not

addressed in the paper. Nonetheless, it is evident that finite temperature and finite cloud length effects can impact the development of the gradient drift instability.

The purpose of this paper is to present a linear stability analysis of the gradient drift instability which incorporates both finite temperature and finite parallel length effects. A simple plasma model is used (similar to the one used in Sperling et al. (1984)) which permits an analytical solution to the dispersion equation. It is found that the short wavelength modes are stabilized by redistribution of electrons parallel to $\underset{\sim}{B}_0$ (i.e., parallel electron diffusion or parallel electron response to the perturbed fields) which neutralize the charge imbalance set up by the instability. An analytical expression for the critical wavenumber for the stabilization of instability is given, as well as numerical results.

The organization of the paper is as follows. In the next section we derive a set of general nonlinear equations which describe the evolution of a three dimensional plasma cloud. In Section III we discuss the equilibrium to be used in the instability analysis. In Section IV we derive a general dispersion equation, and present both analytical and numerical results. Finally, in the last section we summarize our findings and discuss the relevance of our results to cloud structure.

II. GENERAL EQUATIONS

We first derive a set of nonlinear equations to describe the evolution of a warm plasma cloud in a uniform magnetic field $\underset{\sim}{B} = B_0 \hat{z}$ with a background neutral wind $\underset{\sim}{V}_n = V_n \hat{x}$ [see Fig. 1a]. For simplicity we consider only low frequency $\partial/\partial t \ll \nu_\alpha$ motion of the cloud and take the electron collisions to be sufficiently weak so that $\nu_e/\Omega_e \ll 1$ but allow ν_i/Ω_i to be arbitrary. The collision frequency and gyrofrequency of

the α species are given by ν_α and Ω_α, respectively. Both electrons and ions are taken to be warm and for simplicity we consider the isothermal limit. In this case the fundamental equations of our analysis are continuity, momentum transfer, charge neutrality and Ampere's law:

$$\frac{\partial n}{\partial t} + \nabla \cdot (n \underset{\sim}{v}_e) = 0 \tag{1}$$

$$0 = - e\underset{\sim}{E} - \frac{e}{c} \underset{\sim}{v}_e \times \underset{\sim}{B} - m_e \nu_{en} (\underset{\sim}{v}_e - \underset{\sim}{V}_n) - m_e \nu_{ei} (\underset{\sim}{v}_e - \underset{\sim}{v}_i) - \frac{T_e}{n} \nabla n \tag{2}$$

$$0 = e\underset{\sim}{E} + \frac{e}{c} \underset{\sim}{v}_i \times \underset{\sim}{B} - m_i \nu_{in} (\underset{\sim}{v}_i - \underset{\sim}{V}_n) - m_i \nu_{ie} (\underset{\sim}{v}_i - \underset{\sim}{v}_e) - \frac{T_i}{n} \nabla n \tag{3}$$

$$\nabla \cdot \underset{\sim}{J} = \nabla \cdot [n(\underset{\sim}{v}_i - \underset{\sim}{v}_e)] = 0 \tag{4}$$

$$\nabla \times \underset{\sim}{B} = \frac{4\pi}{c} \underset{\sim}{J} \tag{5}$$

where $\underset{\sim}{v}_\alpha$ and T_α are the fluid velocity and temperature of species α, respectively, $\nu_{\alpha n}$ is the α specie-neutral collision frequency, ν_{ei} is the electron-ion collision frequency, ν_{ie} is the ion-electron collision frequency, and α refers to electrons (e) or ions (i). We take the electric and magnetic fields to be represented by potentials as

$$\underset{\sim}{E} = - \nabla\phi - \frac{1}{c} \frac{\partial A_z}{\partial t} \hat{z} \tag{6}$$

and

$$\underset{\sim}{B} = B_0 \hat{z} + \nabla A_z \times \hat{z} \tag{7}$$

where ϕ is the electrostatic potential and A_z is the vector potential associated with the magnetic field produced by the self-consistent plasma currents. We consider only A_z since $J_\parallel \gg J_\perp$ and assume $|\nabla A_z \times \hat{z}| \ll B_0$.

The electron cross-field motion is given by

$$\underset{\sim}{v}_{e\perp} = -\frac{c}{B}\nabla_\perp\phi \times \hat{z} + \frac{cT_e}{eBn}\nabla_\perp n \times \hat{z} \tag{8}$$

while the parallel motion is given by

$$v_{\parallel e} = -\left[eE_\parallel + T_e\nabla_\parallel \ell n(n) + f(\nu_{ei}/\nu_{en})T\nabla_\parallel \ell n(n)\right]/\left[m_e(\nu_e + f\nu_{ei})\right] \tag{9}$$

with

$$E_\parallel = -\nabla_\parallel\phi - \frac{1}{c}\frac{\partial A_z}{\partial t}, \tag{10}$$

where $\nu_e = \nu_{ei} + \nu_{en}$, $\nabla_\parallel = \hat{b}\cdot\nabla$, $\hat{b} = \underset{\sim}{B}/|\underset{\sim}{B}_0|$, and $T = T_e + T_i$. The assumption that $\nu_e/\Omega_e \ll 1$ while $\nu_{in}/\Omega_i \sim 1$ requires that $f \equiv m_e\nu_{en}/m_i\nu_{in} \ll 1$.

The ion cross-field motion is given by

$$\underset{\sim}{v}_{i\perp} = \delta_i\Big[-\frac{c}{B}\nabla_\perp\phi \times \hat{z} + \frac{\nu_{in}}{\Omega_i}\underset{\sim}{v}_n \times \hat{z} - \frac{cT_i}{eBn}\nabla n \times \hat{z}$$

$$- \frac{\nu_{in}}{\Omega_i}\frac{c}{B}\nabla_\perp\phi + \Big(\frac{\nu_{in}}{\Omega_i}\Big)^2\underset{\sim}{v}_n - \frac{\nu_{in}}{\Omega_i}\frac{cT_i}{eBn}\nabla_\perp n\Big], \tag{11}$$

where $\delta_i = (1 + \nu_{in}^2/\Omega_i^2)^{-1}$, and the parallel motion is given by

$$v_{\parallel i} = \{[eE_\parallel + T_e\nabla_\parallel \ell n(n)]\nu_{en} - \nu_e T\nabla_\parallel \ell n(n)\}/[m_i\nu_{in}(\nu_e + f\nu_{ei})]. \tag{12}$$

In (11) we have included both the Pedersen and Hall responses to the electric field, neutral wind and pressure.

Substituting (8)-(12) into (1), (4) and (5) we find that

$$\frac{dn}{dt} - \frac{c}{B} \nabla\hat{\phi} \times \hat{z} \cdot \nabla n + \nabla_{\parallel}\left(\frac{c}{4\pi e} \nabla_{\perp}^2 A_z - D_{\parallel}\nabla_{\parallel} n\right) = 0, \tag{13}$$

$$\delta_i \frac{c}{B} \frac{\nu_{in}}{\Omega_i} \nabla_{\perp} \cdot n\nabla_{\perp}\hat{\phi} + \delta_i \frac{c}{B} \frac{\nu_{in}^2}{\Omega_i^2} \hat{z} \times \nabla\hat{\phi} \cdot \nabla n + \frac{\nu_{in}}{\Omega_i} \hat{z} \times \underset{\sim}{V}_n \cdot \nabla n$$

$$+ D_{\perp}\nabla_{\perp}^2 n + \frac{c}{4\pi e} \nabla_{\parallel}\nabla_{\perp}^2 A_z = 0, \tag{14}$$

$$\nabla_{\perp}^2 A_z = \frac{4\pi}{c\eta_e} \left(\nabla_{\parallel}\hat{\phi} + \frac{1}{c} \frac{dA_z}{dt}\right), \tag{15}$$

where $\eta_e = m_e\nu_e/ne^2$ is the parallel resistivity, $D_{\parallel} = T/m_i\nu_{in}$ and $D_{\perp} = \delta_i(\nu_{in}/\Omega_i)cT/eB$ are the parallel and perpendicular ion transport coefficients, $T = T_e + T_i$, and

$$\hat{\phi} \equiv \phi - \frac{T_e}{e} \ell n(n) - \frac{B}{c} \frac{\nu_{in}}{\Omega_i} \underset{\sim}{V}_n \cdot \underset{\sim}{x}, \tag{16}$$

$$\frac{d}{dt} \equiv \frac{\partial}{\partial t} + \frac{\nu_{in}}{\Omega_i} \hat{z} \times \underset{\sim}{V}_n \cdot \nabla, \tag{17}$$

$$\nabla_{\parallel} = \frac{\partial}{\partial z} + B_0^{-1} \nabla A_z \times \hat{z} \cdot \nabla. \tag{18}$$

Equation (13) is the electron continuity equation, (14) is the charge conservation equation and (15) is Ampere's law. Note that the electron pressure has been absorbed into $\hat{\phi}$ in (16) and that terms of order $f \ll 1$ have been discarded compared with those of order unity. Equations (13)-(18) constitute a complete description of the evolution of a three-dimensional warm plasma cloud.

III. EQUILIBRIUM

We will consider the linear stability of a two-dimensional cloud which is localized both along and across the magnetic field $\underset{\sim}{B}_0$: $n_c = n_c(x, z)$ with $n_c \neq 0$ for $|x| \lesssim x_c$ and $|z| \lesssim z_c$. The background plasma is taken to be uniform throughout the region $|z| < z_b$ between two insulating plates at $z = \pm z_b$. The location of the plates, enables us to control the ratio of the total magnetic-field-line integrated Pedersen conductivity of the cloud to that of the background, $n_c z_c/(n_c z_c + n_b z_b)$. This ratio is an important parameter of the equilibrium configuration.

The equations describing the two dimensional plasma cloud are given by

$$\frac{\partial n}{\partial t} - D_{\parallel} \frac{\partial^2 n}{\partial z^2} + \frac{c}{4\pi e} \frac{\partial}{\partial z} \frac{\partial^2 A_z}{\partial x^2} = 0, \tag{19}$$

$$\delta_i \frac{c}{B} \frac{\nu_{in}}{\Omega_i} \frac{\partial}{\partial x} n \frac{\partial}{\partial x} \hat{\phi} + D_{\perp} \frac{\partial^2 n}{\partial x^2} + \frac{c}{4\pi e} \frac{\partial}{\partial z} \frac{\partial^2 A_z}{\partial x^2} = 0, \tag{20}$$

$$\frac{\partial^2 A_z}{\partial x^2} = \frac{4\pi}{c n_e} \left(\frac{\partial \hat{\phi}}{\partial z} + \frac{1}{c} \frac{\partial A_z}{\partial t}\right). \tag{21}$$

When there are no density gradients in the x direction, the solution to these equations is $\hat{\phi} = -(B/c)(\nu_{in}/\Omega_i) V_n x$ so that

$$\phi = (T_e/e) \ln [n(z)/n_b] \tag{22}$$

with $A_z = 0$, i.e., the potential adjusts itself so that the electrons are in force balance along the magnetic field as the cloud diffuses along $\underset{\sim}{B}_0$. In writing the solution for ϕ in (22) we have required $\phi \to 0$ for $|z| > z_c$ since we have assumed that only the charge accumulations associated with the motion of the plasma cloud itself are responsible for the development of ϕ. There is no charge at $z = \pm z_b$. The density satisfies

$$\partial n/\partial t - D_{\parallel}\partial^2 n/\partial z^2 = 0 \tag{23}$$

so that n diffuses along $\underset{\sim}{B}_0$. In the opposite limit, where there are no density gradients in the z direction ($\partial/\partial z = 0$), $A_z = 0$ and $\hat{\phi} = -(T/e)\ell n(n) - (B/c)(\nu_{in}/\Omega_i)V_n \int_{-\infty}^{x} dx(n_b/n)$ so that

$$\phi = -\frac{T_i}{e}\,\ell n\left[\frac{n(x)}{n_b}\right] + \frac{B}{c}\frac{\nu_{in}}{\Omega_i}V_n \int_{-\infty}^{x} dx\left(1 - \frac{n_b}{n}\right), \tag{24}$$

where we have required $\phi \to 0$ as $|x| \to \infty$. In Eq. (24) the potential adjusts itself so that the perpendicular ion pressure gradient is balanced by the electrostatic field. In comparing the expressions for ϕ in (22) and (24), it is important to note that the electron and ion pressures push the potential in the opposite direction (compare the signs of the terms proportional to T_e and T_i).

We now return to the more general two dimensional equations in (19)-(21). These equations describe three time scales: the resistive flux diffusion time, $\tau_r = 4\pi x_c^2/\eta_e c^2$; the parallel diffusion time, $\tau_{\parallel} = z_c^2/D_{\parallel}$; and the perpendicular diffusion time, $\tau_{\perp} = x_c^2/D_{\perp}$. We assume that the flux diffusion time is the shortest time scale so that inductive effects are not important in the equilibrium, i.e., in Eq. (21) $\partial A_z/\partial t \ll c\,\partial\hat{\phi}/\partial z$. The equations then simplify to

$$\frac{\partial n}{\partial t} - D_{\parallel}\frac{\partial^2 n}{\partial z^2} - D_{\perp}\frac{\partial^2 n}{\partial x^2} - \delta_i \frac{c}{B}\frac{\partial}{\partial x}\, n\,\frac{\partial\hat{\phi}}{\partial x} = 0, \tag{25}$$

$$\delta_i \frac{c}{B}\frac{\nu_{in}}{\Omega_i}\frac{\partial}{\partial x}\, n\,\frac{\partial\hat{\phi}}{\partial x} + \frac{1}{e\eta_e}\frac{\partial^2\hat{\phi}}{\partial z^2} + D_{\perp}\frac{\partial^2 n}{\partial x^2} = 0. \tag{26}$$

I. CONCLUDING REMARKS

We have presented a relatively simple analysis of the gradient drift nstability in barium clouds which includes both finite temperature and inite parallel length effects. We have derived a general set of nonlinear quations which describe the evolution of a three dimensional plasma cloud n the ionosphere. We then investigate the stability of a two dimensional lasma cloud in which the density varies in the direction of the neutral rind and along the ambient magnetic field $\underset{\sim}{B}_0$. By modeling the density 'ariation along $\underset{\sim}{B}_0$ as a waterbag, we are able to obtain an analytic lispersion relation for the gradient drift instability. There is no static :quilibrium since the cloud diffuses both perpendicular and parallel :o $\underset{\sim}{B}_0$ so that we restrict our analysis to time scales short compared to the :loud diffusion time scales.

In recent work Sperling et al. (1984) found that the finite length of the cloud suppressed the growth of long wavelength modes because of "good" coupling to the background plasma. However, the growth rate of short wavelength modes is unaffected by the finite size of the cloud since they do not couple to the background in a zero temperature plasma. In contrast to this result, we find that in a finite temperature plasma the short wavelength modes do couple to the background plasma and that for sufficiently short wavelengths the modes are completely stabilized. Stabilization results as the electrons redistribute parallel to $\underset{\sim}{B}_0$ and neutralize the charge imbalance set up by the instability. The parallel electron motion results from diffusion and/or the response to the perturbed fields. We have also derived a simple analytic expression (see (54)) for the wavenumber corresponding to marginal stability (i.e., $\gamma = 0$). Our results are consistent with previous numerical computations of Sperling and

V. NUMERICAL RESULTS

We now present quantitative results for the wave frequency of the gradient drift instability by solving (43) numerically. In Fig. 2 we plot γ/γ_0 (solid curve) and ω_r/γ_0 (dashed curve) vs. $k_y\rho_s$ where $\omega = \omega_r + i\gamma$ is the wave frequency. We consider the following typical parameters for a barium cloud at 180 km: $n_c/n_b = 10.0$, $T_e = T_i = 0.1$ eV, $m_i = 16\ m_p$ (0^+ background), $z_c = 10$ km, $B = 0.3$ G, $\alpha = 10^6$, $D_\perp = 100$ m^2/sec, $V_n = V_{eff} = 20$ m/sec and $L_n = 1$ km. From these values we note that $c_s = 10^3$ m/sec and $\rho_s = 6$ m. The main features of Fig. 2 are described as follows. First, the growth rate has a maximum value at $k_y\rho_s = k_{ym}\rho_s \simeq 0.08$. For $k_y < k_{ym}$ the growth rate decreases because of coupling to the background plasma as described in Sperling et al. (1984). For $k_y > k_{ym}$ the growth rate decreases rapidly and becomes stable (i.e., $\gamma < 0$). This is due to parallel electron motion as described in the preceding section and is the dominant finite temperature effect. Second, the critical wavenumber for stabilization as given by (54) is denoted by the arrow along the $k_y\rho_s$ axis $(k_y\rho_s \simeq 0.26)$. It is seen that (54) gives a very good approximation to the critical wavenumber obtained numerically $(k_y\rho_s = 0.28)$. For the parameters used the critical wavelength is given by $\lambda_c \simeq 135$ m. Third, the real frequency is linear in k_y and is proportional to the diamagnetic drift velocity $V_d = (cT/eB)(n_c'/n_c)$.

The results shown in Fig. 2 appear to be in qualitative agreement with the numerical work of Sperling and Glassman (1984). They consider a plasma cloud with a Gaussian distribution along the magnetic field rather than a waterbag model. The shape of the curve of γ vs k_y shown in Fig. 2 is similar to corresponding curves presented in their report. Moreover, they also find that $\omega_r \propto k_y$ for large k_y.

with

$$\omega_r = \omega_*\left(1 + \frac{n_c^2}{n_b^2}\frac{2\gamma_0 z_c^2}{\alpha D_\perp}\right)^{-1} \tag{55}$$

where $L_n = -\left(n_c'/n_c\right)^{-1}$ and $\rho_s = c_s/\Omega_i$ is the Larmor radius based on the sound speed $c_s = \left(T/m_i\right)^{1/2}$. Note from (54) that in the limit $T \to 0$, then $k_c \to \infty$ so the mode is not stabilized for a zero temperature plasma [Sperling et al. (1984)]. Equation (54) also appears to imply that k_c becomes very large as the integrated cloud density n_c increases. This result is misleading. In a cloud which is finite in the y direction, the neutral wind velocity V_n in (54) should be replaced by the effective slip velocity V_{eff} of the cloud and the neutral wind. For a circular cloud, the effective velocity is given by [Ossakow and Chaturvedi, 1978]

$$V_{eff} = 2V_n\, n_b z_b/\left(n_b z_b + n_c z_c\right). \tag{56}$$

In the limit of very large $n_c z_c$, Eq. (54) yields the critical wavelength

$$k_c^2 L_n^2 = \frac{4V_n^2 z_b^2}{2D_\perp^2}\left(1 + \frac{4z_b^2 V_n^2}{\alpha\rho_s^2 c_s^2}\right), \tag{57}$$

which is independent of $n_c z_c$. Thus, short wavelength modes are stable even in large ionospheric clouds.

Two significant features of (52) are first that γ_0 does not enter the equation, and second that there appears to be an instability even in the absence of γ_0. However, the unstable root is invalid. In order for $\tilde{\phi}$ to remain bounded as $|z|$ becomes large, we require $\mathrm{Re}(k_b) > 0$. Thus, for $\bar{\gamma} \approx i\omega_*$ we find

$$k_b = (\omega_*/\alpha D_\perp)^{1/2} e^{i\pi/4}. \tag{53}$$

The root with the opposite sign must be discarded. Inserting this expression for k_b into (46), we obtain the damped root in (52). Thus, when thermal effects are retained, the gradient-drift mode is stable for large k_y.

The stabilization mechanism can be understood in terms of our earlier discussion of the local dispersion relation. When ω_* is discarded in (45) and (46), the parallel wavevector k_b remains real (the mode is evanescent in the outer region) and the instability survives even as $k_y \to \infty$. However, when ω_* is retained, the parallel wavevector k_b becomes complex (the mode is evanescent and propagating in the outer region) and the mode is stable for large k_y. In other words, ω_* causes the mode to become oscillatory along $\underset{\sim}{B}$ and the electrons can now move along rather than across $\underset{\sim}{B}$ to neutralize the ions; the mode is therefore stable.

To obtain an expression for the critical wavelength k_c where the mode becomes stable, we take $\bar{\gamma} = -i\omega_r$ and solve (46) directly. The critical wavelength is given by

$$k_c^2\rho_s^2 = \frac{V_n^2}{c_s^2}\left[\left(1 + \frac{2n_c^2 z_c^2}{n_b^2}\frac{V_n}{\alpha D_\perp L_n}\right)^2 + \frac{4n_c^2 z_c^2}{n_b^2}\frac{\rho_s^2 c_s^2}{\alpha D_\perp^2 L_n^2}\right] \tag{54}$$

$$(\gamma_0 - \bar{\gamma})^2 = \alpha \frac{n_b^2 D_r}{n_c^2 z_c^2} \bar{\gamma}, \tag{47}$$

and is independent of the plasma temperature. For $z_c^2 \gg \alpha D_r n_b^2/n_c^2\gamma_0$,

$$\bar{\gamma} \approx \gamma_0 \tag{48}$$

while in the opposite limit $z_c^2 \ll \alpha D_r n_b^2/n_c^2\gamma_0$,

$$\bar{\gamma} = \frac{\gamma_0^2 n_c^2 z_c^2}{\alpha n_b^2 D_r} . \tag{49}$$

These results have been obtained previously [Sperling et al. (1984)].

When k_y becomes very large, $k_b^2 = \bar{\gamma}/\alpha D_\perp$ and the dispersion relation becomes

$$(\bar{\gamma} - i\omega_* - \gamma_0)^2 = \alpha D_\perp \frac{n_b^2}{n_c^2 z_c^2} \bar{\gamma}. \tag{50}$$

For large k_y, we have $\omega_* \gg \gamma_0$ since $\omega_* \propto k_y$ and therefore to lowest order

$$\bar{\gamma} = i\omega_*, \tag{51}$$

the mode simply propagates at the diamagnetic frequency. To investigate whether the mode is stable or unstable in this limit, corrections to this result must be calculated. These corrections arise from the right side of (50) and yield the eigenvalue

$$\bar{\gamma} = i\omega_* \pm \frac{n_b}{n_c z_c} (\alpha D_\perp \omega_*)^{1/2} e^{i\pi/4}. \tag{52}$$

where

$$\frac{k_b}{k_c} = \left[\frac{n_b}{n_c} \frac{\bar{\gamma}}{\gamma_0 - \bar{\gamma} + i\omega_*}\right]^{1/2}. \tag{44}$$

In Sperling et al. (1984), the dispersion relation was carefully solved in all possible limits of the various parameters. In order to clearly emphasize the role of finite temperature in stabilizing short wavelength modes, we will focus our analysis primarily on modes with growth rates less than γ_0 for which $k_b/k_c \ll 1$. In this limit (43) becomes

$$k_c^2 z_c = k_b \tag{45}$$

or

$$n_c z_c (\bar{\gamma} - i\omega_* - \gamma_0) + n_b k_b^{-1} \bar{\gamma} = 0. \tag{46}$$

In the form shown in (46), the nature of the dispersion relation can be simply understood. The first (second) term is the magnetic field line integrated contribution from the cloud (background). The background contribution arises only from the region $|z| < k_b^{-1}$ since the perturbed potential $\tilde{\phi}$ is small outside of this interval. The result in (46) can be directly obtained by integrating (33) for $\tilde{\phi}$ along z.

The dispersion relation in (45) or (46) can be solved analytically for various values of k_y. In the limit $k_y \to 0$, $k_b^2 = \bar{\gamma}/\alpha D_r$ and the dispersion relation is given by

discontinuity in the density at $z = \pm z_c$, we find that $\tilde{\tilde{\phi}}$ and $\tilde{A}_z$ must be continuous. For the even $\tilde{\tilde{\phi}}$ solution $(\tilde{\tilde{\phi}}_c^2 = 0)$, we obtain the dispersion equation

$$k_c z_c = \tan^{-1}\left[\frac{k_b}{k_c}\frac{\bar{\gamma} + k_y^2 D_{rc}}{\bar{\gamma} + k_y^2 D_{rb}}\right] + m\pi \tag{42}$$

where m is an integer. The dispersion relation for the odd $\tilde{\phi}$ mode $(\tilde{\tilde{\phi}}_c^1 = 0)$ is similar to (42) except $\tan^{-1}$ is replaced by $-\cot^{-1}$. The result in (42) is identical to the dispersion relation obtained previously by Sperling et al. (1984) except that the expressions for k_b and k_c given in (40d) and (41d) now contain thermal effects which were previously neglected.

In general, the dispersion equation (42) has an infinite number of solutions for a given set of physical parameters, corresponding to eigenmodes with an increasing number of nodes (m) along z. The dispersion equation (42) can be solved numerically for arbitrary values of the background and cloud parameters. However, to gain an understanding of the general scaling of the growth rate γ with the parallel extent of the cloud and temperature, it is useful to solve (42) analytically. To do this we make a number of simplifying assumptions. We consider only the lowest order mode (i.e., $m = 0$ which implies $0 < k_c z_c < \pi/2$; it is easily shown that this mode has the largest growth rate); take ν_{in}/Ω_i to be small so that take all parameters but the density to be the same inside and outside of the cloud; assume $n_c >> n_b$; and $\nu_{ei} >> \nu_{en}$ so that the resistive diffusion coefficient is continuous across the boundary $z = z_c$ (i.e. $D_{rb} = D_{rc}$). With these assumptions the dispersion equation becomes

$$k_c z_c = \tan^{-1}(k_b/k_c) \tag{43}$$

with

$$(\bar{\gamma}_b + k_y^2 D_{rb})\tilde{A}_{zb} = k_b c \tilde{\tilde{\phi}}_b \tag{40c}$$

$$k_b^2 = \frac{\bar{\gamma}(\bar{\gamma} + k_y^2 D_r)}{\alpha D_r (\bar{\gamma} + k_y^2 D_\perp)} \Big|_b \tag{40d}$$

where the subscript b on a given parameter indicates that it is to be evaluated in the region $|z| > z_c$. Note that we have assumed $k_b z_b \gg 1$ and that solutions which diverge as z becomes large have been omitted from (40). This assumption is consistent with the approximation $z_b \ll \alpha^{1/2} x_c$ made in deriving the equilibrium potential ϕ as long as $k_b z_b \gg 1$.

In the region $|z| < z_c$ the solutions for $\hat{\phi}$ and $\tilde{A}_z$ are

$$\tilde{A}_z = \tilde{A}_{zc}^1 \sin(k_c z) - \tilde{A}_{zc}^2 \cos(k_c z) \tag{41a}$$

$$\tilde{\tilde{\phi}} = \tilde{\tilde{\phi}}_c^1 \cos(k_c z) + \tilde{\tilde{\phi}}_c^2 \sin(k_c z) \tag{41b}$$

with

$$(\bar{\gamma}_c + k_y^2 D_{rc})\tilde{A}_{zc}^{1,2} = k_c c \tilde{\tilde{\phi}}_c^{1,2} \tag{41c}$$

$$k_c^2 = -\frac{(\bar{\gamma} - i\omega_* - \gamma_0)(\bar{\gamma} + k_y^2 D_r)}{\alpha D_r (\bar{\gamma} + k_y^2 D_\perp)} \Big|_c \tag{41d}$$

We note that in writing (40d) and (41d) we have assumed $\bar{\gamma} \gg k_y \bar{V}_i$ for simplicity.

To complete the dispersion relation, we must match the various plane wave solutions at $z = \pm z_c$. The appropriate matching conditions are obtained from (32) and (33). Integrating these two equations across the

where $D_{\perp i} = \delta_i(\nu_{in}/\Omega_i)cT_i/eB$. In the limit $k_z = 0$, $\tilde{n}_e = (ik_y cn'/\gamma B)\tilde{\phi}$ and the usual growth rate of the instability is obtained by equating $\tilde{n}_e$ and $\tilde{n}_i$. In this case the density perturbation $\tilde{n}_e$ and the electric field perturbation, $\tilde{E}_y = -ik_y\tilde{\phi}$, are in phase and the usual physical description of instability applies. However, in the limit of large k_z with $T_e \neq 0$, $\tilde{n}_e = n_0 e\tilde{\phi}/T_e$, i.e., the electrons are adiabatic and neutralize the ions by moving along $\underset{\sim}{B}$ rather than across $\underset{\sim}{B}$. In this case $\tilde{n}_e$ is out of phase with $\tilde{E}_y$ and there is no instability. When $T_e = 0$ and k_z is large, the mechanism is somewhat different although the mode is also stable. In this case, the electrons bunch parallel to $\underset{\sim}{B}$, and $\tilde{n}_e = (k_z^2/en_e\gamma)\tilde{\phi}$. For k_z large the ions can only neutralize the electrons if $\gamma = -k_y^2 D_{\perp i} + ik_y V_n \nu_{in}/\Omega_i$. Namely, the electrons bunch parallel to $\underset{\sim}{B}$ and the ions diffuse across $\underset{\sim}{B}$ to neutralize the charge imbalance. Finally, we note that while electron parallel diffusion or ion perpendicular diffusion stabilizes the mode when the perturbation is periodic along $\underset{\sim}{B}$, when the spatial dependence of the mode is exponential, i.e., $\tilde{p}(z) \sim \tilde{p}\exp(\pm k_z z)$, the thermal effects are not stabilizing. The distinction between a periodic and a nonperiodic solution is important in interpreting the dispersion relation which is obtained for the equilibrium shown in Fig. 1b.

We now solve (32) and (33) for the profile given by (19). The boundary conditions used are $\tilde{\tilde{\phi}}$, $\tilde{A}_z \to 0$ as $|z| \to z_m$. For the step profile for $n(x,z)$ the solutions to (32) and (33) in the region $|z| > z_c$ can be written as plane waves

$$\tilde{A}_z = \tilde{A}_{zb}\exp\left[-k_b|z|\right] \tag{40a}$$

$$\tilde{\phi} = \tilde{\phi}_b\exp\left[-k_b|z|\right] \tag{40b}$$

$$\gamma = \left(\gamma_0 - \frac{k_z^2 T}{m_e \nu_e}\right)\left(\frac{k_y^2 D_r}{k_y^2 D_r + k_z^2 V_A^2/\nu_{in}\delta_i}\right) \tag{36}$$

The Alfvén wave has a stabilizing influence on the instability in the electromagnetic limit but thermal effects do not affect the growth rate. Of course, the gradient drift instability is not stable when $k_z V_A^2/\nu_{in}\delta_i > \gamma_0$ as might be construed from (35) since the expression for γ given in (35) breaks down when $\gamma < k_y^2 D_r$. Thermal effects can have a significant influence on the growth rate when $\gamma < k_y^2 D_r$ (electrostatic limit). Namely, for

$$k_z^2 T/m_e \nu_e < \gamma_0, \tag{37}$$

the electrons can move a wavelength along $\underset{\sim}{B}$ during the growth time of the instability, and the mode is stable. In the limit of $k_z \to \infty$ in (36),

$$\gamma = - k_y^2 D_\perp \tag{38}$$

so that the mode damps at the ion diffusion rate.

The stabilization mechanism can be understood by examining the electron and ion density perturbations in the electrostatic limit,

$$\tilde{n}_e = \frac{\left(ik_y cn'/B + k_z^2/e\eta_e\right)}{\gamma + k_z^2 T_e/m_e \nu_e}\,\tilde{\phi} \tag{39a}$$

$$\tilde{n}_i = \frac{\left[ik_y cn'/B - k_y^2 c(\nu_{in}/\Omega_i)n/B\right]}{\gamma + k_y^2 D_{\perp i} - ik_y V_n \nu_{in}/\Omega_i}\,\tilde{\phi} \tag{39b}$$

In deriving (32) and (33) we have neglected parallel ion diffusion as discussed previously and assumed $n_c >> n_b$. The primes denote a derivative with respect to x. The important finite temperature effects that appear in (32) and (33) are the diamagnetic drift frequency (ω_*), perpendicular ion diffusion $(D_\perp)$, and modification of the equilibrium $(\hat{\phi}_0')$. In the limit $T_i = T_e = 0$, Eqs. (32) and (33) reduce to those previously derived by Sperling et al. (1984). The eigenvalue $\bar{\gamma}$ is in a frame of reference moving with the electron fluid.

Prior to solving (32) and (33) for the density profile shown in Fig. 1b, we first consider a cloud of infinite extent $[z_c \to \infty]$ and Fourier expand in the direction parallel to $\underset{\sim}{B}_0$, i.e., $\tilde{p}(z) \sim \tilde{p} \exp[ik_z z]$. This allows insight into the influence of finite temperature and parallel dynamics on the instability. The local dispersion equation is given by

$$(\bar{\gamma} - i\omega_* - \gamma_0)(\bar{\gamma} + k_y^2 D_r) = -\frac{k_z^2 V_A^2}{\nu_{in}\delta_i}(\bar{\gamma} - ik_y\bar{V}_i + k_y^2 D_\perp), \tag{34}$$

where $V_A = B/(4\pi n m_i)^{1/2}$ is the Alfvén velocity. This dispersion relation illustrates the coupling between the gradient drift instability and the Alfvén wave when $k_z \neq 0$.

For simplicity, we neglect the terms in (34) which cause the mode to propagate $(\omega_r,\ k_y\bar{V}_i \to 0$ and $\bar{\gamma} \to \gamma)$ and note that $D_r >> D_\perp$ in ionospheric applications. The growth rate can be easily obtained in two limits: in the electromagnetic limit $(\gamma >> k_y^2 D_r)$,

$$\gamma = \gamma_0 - k_z^2 V_A^2/\nu_{in}\delta_i, \tag{35}$$

while in the electrostatic limit $(\gamma << k_y^2 D_r)$

When the electron parallel conductivity is large, $k_\parallel$ is typically quite small so that these inequalities are easily satisfied. Finally, the time evolution of the equilibrium should have a negligible influence on the stability analysis providing

$$|\gamma\tau_\parallel|,\ |\gamma\tau_\perp| \ll 1$$

where γ is the growth (damping) rate of the mode of interest.

IV. LINEARIZED EQUATIONS AND DISPERSION EQUATION

To determine the influence of finite temperature and parallel dynamics on the gradient drift instability we linearize (13)-(15) using the equilibrium discussed in the preceding section. We assume perturbed quantities to vary as $\tilde{p} \sim \tilde{p}(z) \exp(\gamma t + ik_y y)$. After eliminating $\tilde{n}$ algebraically from (13)-(15), we obtain two coupled differential equations for $\tilde{\tilde{\phi}}$ and $\tilde{A}_z$:

$$(\bar{\gamma} + k_y^2 D_r)\tilde{A}_z = - c \frac{\partial \tilde{\tilde{\phi}}}{\partial z} \tag{32}$$

$$(\bar{\gamma} - i\omega_* - \gamma_0)\tilde{\tilde{\phi}} = - \alpha D_r (\bar{\gamma} - ik_y \bar{V}_i + k_y^2 D_\perp) \frac{1}{c} \frac{\partial \tilde{A}_z}{\partial z} \tag{33}$$

where $\bar{\gamma} = \gamma + i(c/B)k_y \hat{\phi}_0'$, $\tilde{\tilde{\phi}} = \tilde{\phi} - (T_e/e)\, \ell n\, \tilde{n}$, $D_r = \nu_e c^2/\omega_{pe}^2$, $\bar{V}_i = (\nu_{in}/\Omega_i)\delta_i \bar{V}_n$, $\alpha = (\Omega_e/\nu_e)(\Omega_i/\nu_{in})\delta_i^{-1}$, $\omega_* = - k_y(cT/eB)(n_c'/n_c)$, $\bar{V}_n = V_n + (c/B)(\nu_{in}/\Omega_i)\hat{\phi}_0'$, $\gamma_0 = - (n_c'/n_c)\bar{V}_n$, and

$$\hat{\phi}_0' = \left(\frac{B}{c} \frac{\nu_{in}}{\Omega_i} V_n - \frac{T}{e} \frac{n_c'}{n_c}\right) \frac{n_c z_c}{n_c z_c + n_b z_b} .$$

$$\frac{\partial \Delta n}{\partial t} - D_{\parallel} \frac{\partial^2 \Delta n}{\partial z^2} - D_{\perp} \frac{\partial^2 \Delta n}{\partial x^2} - \delta_i \frac{c}{B} \frac{\partial}{\partial x} \Delta n \frac{\partial \bar{\phi}}{\partial x} = 0,$$

$$\frac{1}{e n_e} \frac{\partial^2 \Delta \hat{\phi}}{\partial z^2} = - D_{\perp} \frac{\partial^2 \Delta n}{\partial x^2} - \delta_i \frac{c}{B} \frac{\nu_i}{\Omega_i} \frac{\partial}{\partial x} \Delta n \frac{\partial \bar{\phi}}{\partial x},$$

where $\Delta\hat{\phi} << \bar{\phi}$. The equation for Δn has no steady state solution so Δn will generally evolve on a time scale of order $\tau_{\parallel} \sim \tau_{\perp}$. The z dependent potential $\Delta\hat{\phi}$ drives an equilibrium current $J_z = n_e^{-1} \partial \Delta\hat{\phi}/\partial z$ which is required so that $\nabla \cdot \underset{\sim}{J} = 0$. The time variation of the equilibrium and the equilibrium parallel current J_z will be neglected when we carry out the linear stability analysis.

Specifically, in the linear stability analysis we formally take the limit $D_{\parallel} \to 0$ and choose

$$n(x,z) = \begin{cases} n_c(x) + n_b & |z| < z_c \\ n_b & z_b > |z| > z_c \end{cases} \tag{31}$$

as shown in Fig. 1b. The perpendicular diffusion coefficient is retained in the stability analysis. The step function model for the density is valid as long as the parallel wavelengths of the modes of interest are much longer than the actual parallel equilibrium density scale length, i.e.,

$$k_{\parallel}^2 z_c^2 << 1.$$

The neglect of the equilibrium parallel current and parallel diffusion can similarly be justified for

$$k_{\parallel} J_z / ne << \omega$$

$$k_{\parallel}^2 D_{\parallel} << \omega,$$

Equation (25) governs the time evolution of n while (26) determines $\hat{\phi}$. For $z_b^2 \ll x_c^2 \, \Omega_e \Omega_i / \nu_e \nu_{in}$, the second term in (26) is much larger than the remaining terms unless $\partial\hat{\phi}/\partial z \approx 0$. Thus, $\hat{\phi}$ is nearly constant along $\underset{\sim}{B}_0$. An equation for $\bar{\hat{\phi}}$ can then be obtained by averaging (25) and (26) along $\underset{\sim}{B}_0$. The resulting equations are

$$\partial \bar{n}/\partial t = 0 \tag{27}$$

$$\frac{\partial}{\partial x} \bar{n} \frac{\partial \bar{\hat{\phi}}}{\partial x} + \frac{T}{e} \frac{\partial^2 \bar{n}}{\partial x^2} = 0 \tag{28}$$

where the average $\bar{p}$ of a function p(z) is defined as

$$\bar{p} = \int_{-z_b}^{z_b} dz \; p(z)/2z_b. \tag{29}$$

Thus, the integrated density $\bar{n}$ is a constant in time. From (28), we obtain an expression for the potential,

$$\phi = \frac{T_e}{e} \ln \left(\frac{n}{n_b}\right) - \frac{T}{e} \ln \left(\frac{\bar{n}}{n_b}\right) + \frac{B}{c} \frac{\nu_{in}}{\Omega_i} V_n \int_{-\infty}^{x} dx \left(1 - \frac{n_b}{\bar{n}}\right). \tag{30}$$

The first and second terms in (30) compete in forcing the potential to balance the parallel electron pressure and ion perpendicular pressure, respectively. In the limit in which n is constant along $\underset{\sim}{B}_0$, $\bar{n} = n$ and $\phi \sim -(T_i/e) \ln (n/n_b)$ so that ϕ balances the ion pressure. In opposite limit, where $z_b/z_c \to \infty$, $\bar{n} = n_b$ and $\phi \sim (T_e/e) \ln (n/n_b)$ so ϕ balances the electron pressure.

Finally, subtracting the field line average of (25) and (26) from itself, we obtain an equation for $\Delta n = n - \bar{n}$ and $\Delta\hat{\phi} = \hat{\phi} - \bar{\hat{\phi}}$,

Glassman (1984) who also noted the importance of finite temperature on the stability of the gradient drift mode.

The extent to which the work described here may have relevance to the barium cloud "freezing" phenomenon deserves some discussion. Briefly, it is observed that barium ion clouds released at ionospheric altitudes will, through the nonlinear evolution of the gradient drift instability, break into smaller pieces. This process, known as bifurcation, continues until a certain minimum transverse dimension is reached, at which point further bifurcation ceases. This frozen scale size is observed to be approximately 400 m. Simple two dimensional models of barium cloud evolution fail to explain frozen scale sizes this large [McDonald et al, 1981]. One explanation which has been advanced to explain freezing is that of end-shorting [Francis and Perkins, 1975; Zalesak et al., 1984] which takes into account the distribution of plasma along magnetic field lines, finite plasma temperature, and parallel currents, as we have done here. However end-shorting depends on the "mapping" of transverse electric fields over relatively large distances along $\underline{B}$; this becomes increasingly more difficult as k increases. Indeed, as shown here, and in Sperling et al. (1984), end-shorting fails to provide stabilization of the very high k modes (at least for the simple profiles of n_c, n_b and ν_{in} considered). If nothing else, the present work shows the existence of a viable stabilization mechanism (i.e., finite temperature) in the gap missed by the end-shorting mechanism. It should also be pointed out, however, that we are not that far removed (135 m stabilization wavelength) from offering a mechanism that by itself may stabilize a 400 m diameter barium striation.

Given the uncertainties in applying a linear theory to explain a complex nonlinear phenomena, the stabilization of the gradient drift instability by parallel electron diffusion must be considered as a strong candidate to explain striation freezing.

ACKNOWLEDGMENT

This research has been supported by the Defense Nuclear Agency.

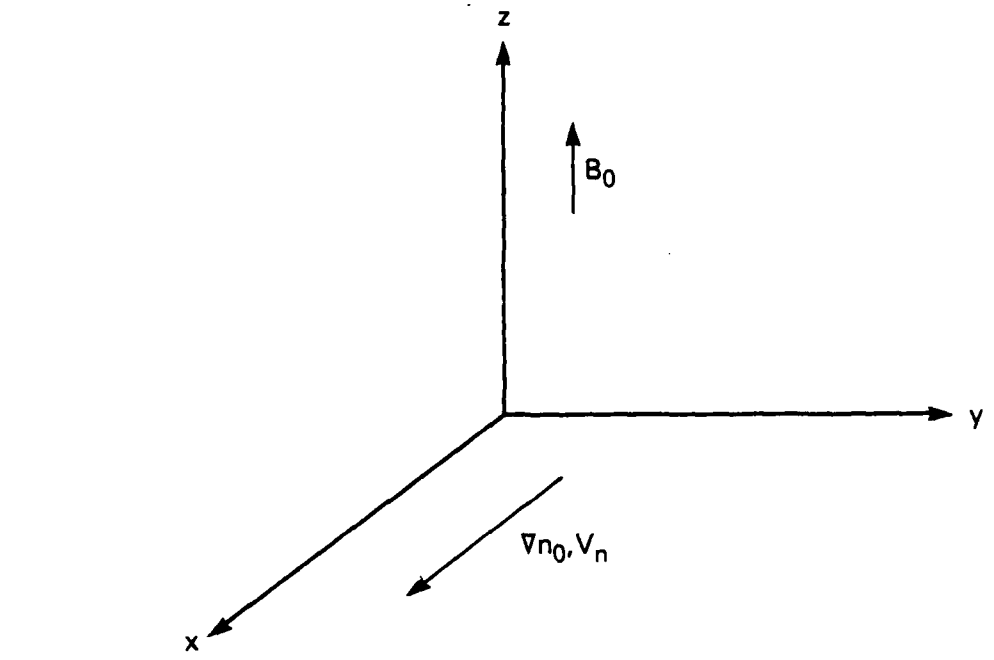

(a)

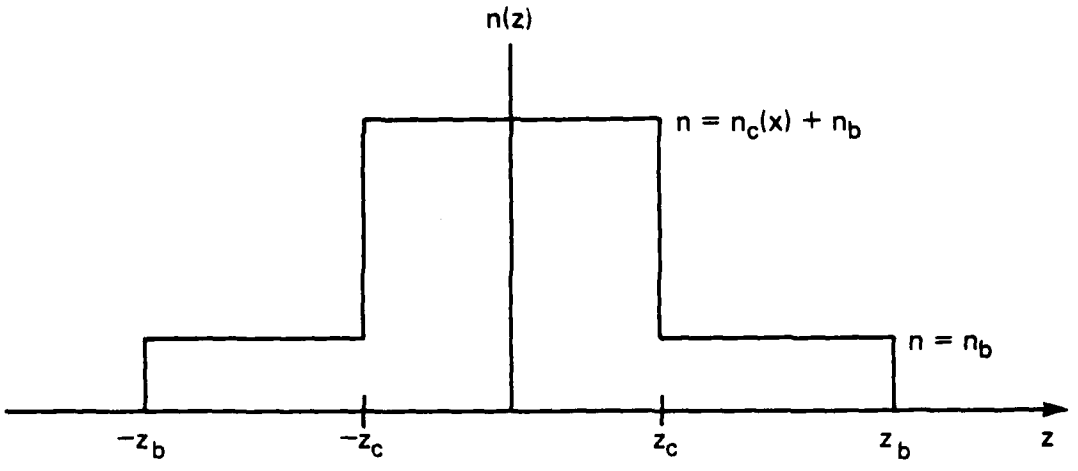

(b)

Fig. 1 Slab geometry and plasma model used in the analysis.

(a) Geometry and plasma configuration.

(b) Cloud and background density profile.

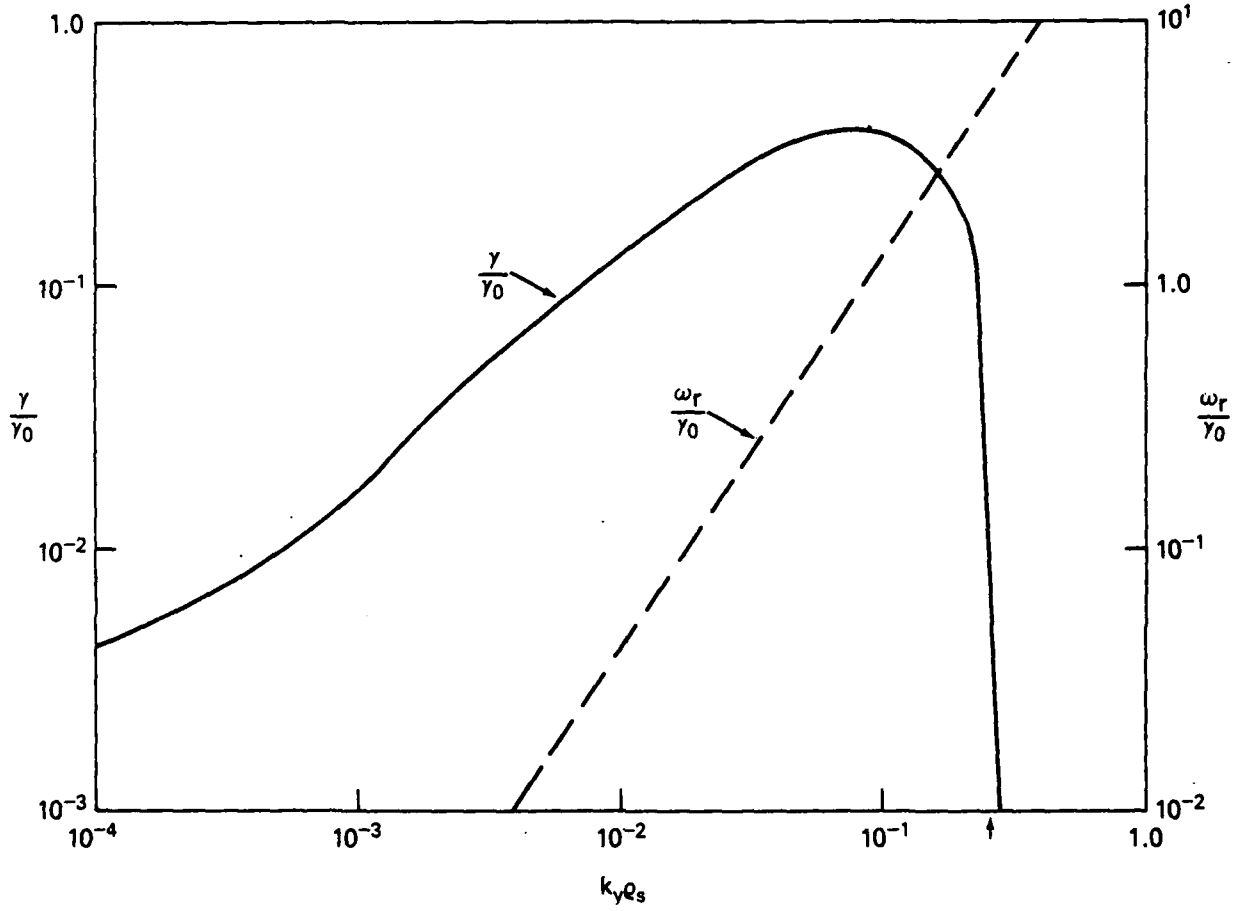

Fig. 2 Plot of ω_r/ω_0 (dashed curve) and γ/γ_0 (solid curve) vs. $k_y\rho_s$ where $\omega = \omega_r + i\gamma$. Parameters used are described in text.

REFERENCES

Chaturvedi, P.K., and S.L. Ossakow, Nonlinear stabilization of the E × B gradient drift instability in ionospheric plasma clouds, J. Geophys. Res., 84, 419, 1979.

Francis, S.H., and F.W. Perkins, Determination of striation scale sizes for plasma clouds in the ionosphere, J. Geophys. Res., 80, 3111, 1975.

Goldman, S.R., L. Baker, S.L. Ossakow, and A.J. Scannapieco, Striation formation associated with barium clouds in an inhomogeneous ionosphere, J. Geophys. Res., 81, 5097, 1976.

Hoh, F.C., Instability of Penning-type discharges, Phys. Fluids, 6, 1184, 1963.

Huba, J.D., S.L. Ossakow, P. Satyanarayana, and P.N. Guzdar, Linear theory of the E × B instability with an inhomogeneous electric field, J. Geophys. Res., 88, 425, 1983.

Keskinen, M.J., S.L. Ossakow, and P.K. Chaturvedi, Preliminary report of numerical simulations of intermediate wavelength E × B gradient drift instability in ionospheric plasma clouds, J. Geophys. Res., 85, 3485, 1980.

Linson, L.M., and J.B. Workman, Formation of striations in ionospheric plasma clouds, J. Geophys. Res., 75, 321, 1970.

McDonald, B.E., M.J. Keskinen, S.L. Ossakow, and S.T. Zalesak, Computer simulation of gradient drift instability processes in Operation Avefria, J. Geophys. Res., 85, 2143, 1980.

McDonald, B.E., S.L. Ossakow, S.T. Zalesak, and N.J. Zabusky, Scale sizes and lifetimes of F region plasma cloud striations as determined by the condition of marginal stability, J. Geophys. Res., 86, 5775, 1981.

Ossakow, S.L. and P.K. Chaturvedi, Morphological studies of rising equatorial spread F bubbles, J. Geophys. Res., 83, 2085, 1978.

Perkins, F.W., and J.H. Doles III, Velocity shear and the E × B instability, J. Geophys. Res., 80, 211, 1975.

Perkins, F.W., N.J. Zabusky, and J.H. Doles III, Deformation and striation of plasma clouds in the ionosphere, 1, J. Geophys. Res., 78, 697, 1973.

Scannapieco, A.J., S.L. Ossakow, S.R. Goldman, and J.M. Pierre, Plasma cloud late time striation spectra, J. Geophys. Res., 81, 6037, 1976.

Shiau, J.N., and A. Simon, Onset of striations in barium clouds, Phys. Rev. Lett., 29, 1664, 1972.

Simon, A., Instability of a partially ionized plasma in crossed electric and magnetic fields, Phys. Fluids, 6, 382, 1963.

Sperling, J.L., and A.J. Glassman, Striation eigenmodes along the geomagnetic field and eigenvalues in the limit of strong ion-neutral collisions, JAYCOR Report J530-83-135, JAYCOR, San Diego, CA, 1983.

Sperling, J.L., J.F. Drake, S.T. Zalesak, and J.D. Huba, "The role of finite parallel length on the stability of barium clouds," J. Geophys. Res., 89, 10913, 1984.

Volk, H.J., and G. Haerendel, Striation in ionospheric clouds, J. Geophys. Res., 76, 454, 1971.

Zabusky, N.J., J.H. Doles III, and F.W. Perkins, Deformation and striation of plasma clouds in the ionosphere, 2, Numerical simulation of a nonlinear two-dimensional model, J. Geophys. Res., 78, 711, 1973.

Zalesak, S.T., P.K. Chaturvedi, S.L. Ossakow, and J.A. Fedder, Finite temperature effects on the evolution of ionospheric barium clouds in the presence of a conducting background ionosphere I. A high altitude incompressible background ionosphere, Memo Report 5346, Naval Res. Lab., Washington, D.C., July 1984.

DISTRIBUTION LIST

DEPARTMENT OF DEFENSE

ASSISTANT SECRETARY OF DEFENSE
COMM, CMD, CONT 7 INTELL
WASHINGTON, D.C. 20301

DIRECTOR
COMMAND CONTROL TECHNICAL CENTER
PENTAGON RM BE 685
WASHINGTON, D.C. 20301
01CY ATTN C-650
01CY ATTN C-312 R. MASON

DIRECTOR
DEFENSE ADVANCED RSCH PROJ AGENCY
ARCHITECT BUILDING
1400 WILSON BLVD.
ARLINGTON, VA. 22209
01CY ATTN NUCLEAR MONITORING RESEARCH
01CY ATTN STRATEGIC TECH OFFICE

DEFENSE COMMUNICATION ENGINEER CENTER
1860 WIEHLE AVENUE
RESTON, VA. 22090
01CY ATTN CODE R410
01CY ATTN CODE R812

DEFENSE TECHNICAL INFORMATION CENTER
CAMERON STATION
ALEXANDRIA, VA. 22314
02CY

DIRECTOR
DEFENSE NUCLEAR AGENCY
WASHINGTON, D.C. 20305
01CY ATTN STVL
04CY ATTN TITL
01CY ATTN DDST
03CY ATTN RAAE

COMMANDER
FIELD COMMAND
DEFENSE NUCLEAR AGENCY
KIRTLAND, AFB, NM 87115
01CY ATTN FCPR

DEFENSE NUCLEAR AGENCY
SAO/DNA
BUILDING 20676
KIRTLAND AFB, NM 87115
01CY D.C. THORNBURG

DIRECTOR
INTERSERVICE NUCLEAR WEAPONS SCHOOL
KIRTLAND AFB, NM 87115
01CY ATTN DOCUMENT CONTROL

JOINT CHIEFS OF STAFF
WASHINGTON, D.C. 20301
01CY ATTN J-3 WWMCCS EVALUATION OFFICE

DIRECTOR
JOINT STRAT TGT PLANNING STAFF
OFFUTT AFB
OMAHA, NB 68113
01CY ATTN JSTPS/JLKS
01CY ATTN JPST G. GOETZ

CHIEF
LIVERMORE DIVISION FLD COMMAND DNA
DEPARTMENT OF DEFENSE
LAWRENCE LIVERMORE LABORATORY
P.O. BOX 808
LIVERMORE, CA 94550
01CY ATTN FCPRL

COMMANDANT
NATO SCHOOL (SHAPE)
APO NEW YORK 09172
01CY ATTN U.S. DOCUMENTS OFFICER

UNDER SECY OF DEF FOR RSCH & ENGRG
DEPARTMENT OF DEFENSE
WASHINGTON, D.C. 20301
01CY ATTN STRATEGIC & SPACE SYSTEMS (OS)

WWMCCS SYSTEM ENGINEERING ORG
WASHINGTON, D.C. 20305
01CY ATTN R. CRAWFORD

COMMANDER/DIRECTOR
ATMOSPHERIC SCIENCES LABORATORY
U.S. ARMY ELECTRONICS COMMAND
WHITE SANDS MISSILE RANGE, NM 88002
01CY ATTN DELAS-EO, F. NILES

DIRECTOR
BMD ADVANCED TECH CTR
HUNTSVILLE OFFICE
P.O. BOX 1500
HUNTSVILLE, AL 35807
01CY ATTN ATC-T MELVIN T. CAPPS
01CY ATTN ATC-O W. DAVIES
01CY ATTN ATC-R DON RUSS

PROGRAM MANAGER
BMD PROGRAM OFFICE
5001 EISENHOWER AVENUE
ALEXANDRIA, VA 22333
01CY ATTN DACS-BMT J. SHEA

CHIEF C-E- SERVICES DIVISION
U.S. ARMY COMMUNICATIONS CMD
PENTAGON RM 1B269
WASHINGTON, D.C. 20310
01CY ATTN C- E-SERVICES DIVISION

COMMANDER
FRADCOM TECHNICAL SUPPORT ACTIVITY
DEPARTMENT OF THE ARMY
FORT MONMOUTH, N.J. 07703
01CY ATTN DRSEL-NL-RD H. BENNET
01CY ATTN DRSEL-PL-ENV H. BOMKE
01CY ATTN J.E. QUIGLEY

COMMANDER
U.S. ARMY COMM-ELEC ENGRG INSTAL AGY
FT. HUACHUCA, AZ 85613
01CY ATTN CCC-EMEO GEORGE LANE

COMMANDER
U.S. ARMY FOREIGN SCIENCE & TECH CTR
220 7TH STREET, NE
CHARLOTTESVILLE, VA 22901
01CY ATTN DRXST-SD

COMMANDER
U.S. ARMY MATERIAL DEV & READINESS CMD
5001 EISENHOWER AVENUE
ALEXANDRIA, VA 22333
01CY ATTN DRCLDC J.A. BENDER

COMMANDER
U.S. ARMY NUCLEAR AND CHEMICAL AGENCY
7500 BACKLICK ROAD
BLDG 2073
SPRINGFIELD, VA 22150
01CY ATTN LIBRARY

DIRECTOR
U.S. ARMY BALLISTIC RESEARCH
LABORATORY
ABERDEEN PROVING GROUND, MD 21005
01CY ATTN TECH LIBRARY,
EDWARD BAICY

COMMANDER
U.S. ARMY SATCOM AGENCY
FT. MONMOUTH, NJ 07703
01CY ATTN DOCUMENT CONTROL

COMMANDER
U.S. ARMY MISSILE INTELLIGENCE AGENCY
REDSTONE ARSENAL, AL 35809
01CY ATTN JIM GAMBLE

DIRECTOR
U.S. ARMY TRADOC SYSTEMS ANALYSIS
ACTIVITY
WHITE SANDS MISSILE RANGE, NM 88002
01CY ATTN ATAA-SA
01CY ATTN TCC/F. PAYAN JR.
01CY ATTN ATTA-TAC LTC J. HESSE

COMMANDER
NAVAL ELECTRONIC SYSTEMS COMMAND
WASHINGTON, D.C. 20360
01CY ATTN NAVALEX 034 T. HUGHES
01CY ATTN PME 117
01CY ATTN PME 117-T
01CY ATTN CODE 5011

COMMANDING OFFICER
NAVAL INTELLIGENCE SUPPORT CTR
4301 SUITLAND ROAD, BLDG. 5
WASHINGTON, D.C. 20390
01CY ATTN MR. DUBBIN STIC 12
01CY ATTN NISC-50
01CY ATTN CODE 5404 J. GALET

COMMANDER
NAVAL OCCEAN SYSTEMS CENTER
SAN DIEGO, CA 92152
01CY ATTN J. FERGUSON

NAVAL RESEARCH LABORATORY
WASHINGTON, D.C. 20375
01CY ATTN CODE 4700 S. L. Ossakow
26 CYS IF UNCLASS. 1 CY
IF CLASS)
01CY ATTN CODE 4701 I Vitkovitsky
01CY ATTN CODE 4780 J. Huba (50
CYS IF UNCLASS, 1 CY IF CLASS)
01CY ATTN CODE 7500
01CY ATTN CODE 7550
01CY ATTN CODE 7580
01CY ATTN CODE 7551
01CY ATTN CODE 7555
01CY ATTN CODE 4730 E. MCLEAN
01CY ATTN CODE 4108
01CY ATTN CODE 4730 B. RIPIN
20CY ATTN CODE 2628

COMMANDER
NAVAL SPACE SURVEILLANCE SYSTEM
DAHLGREN, VA 22448
01CY ATTN CAPT J.H. BURTON

OFFICER-IN-CHARGE
NAVAL SURFACE WEAPONS CENTER
WHITE OAK, SILVER SPRING, MD 20910
01CY ATTN CODE F31

DIRECTOR
STRATEGIC SYSTEMS PROJECT OFFICE
DEPARTMENT OF THE NAVY
WASHINGTON, D.C. 20376
01CY ATTN NSP-2141
01CY ATTN NSSP-2722 FRED WIMBERLY

COMMANDER
NAVAL SURFACE WEAPONS CENTER
DAHLGREN LABORATORY
DAHLGREN, VA 22448
01CY ATTN CODE DF-14 R. BUTLER

OFFICER OF NAVAL RESEARCH
ARLINGTON, VA 22217
01CY ATTN CODE 465
01CY ATTN CODE 461
01CY ATTN CODE 402
01CY ATTN CODE 420
01CY ATTN CODE 421

COMMANDER
AEROSPACE DEFENSE COMMAND/DC
DEPARTMENT OF THE AIR FORCE
ENT AFB, CO 80912
01CY ATTN DC MR. LONG

COMMANDER
AEROSPACE DEFENSE COMMAND/XPD
DEPARTMENT OF THE AIR FORCE
ENT AFB, CO 80912
01CY ATTN XPDQQ
01CY ATTN XP

AIR FORCE GEOPHYSICS LABORATORY
HANSCOM AFB, MA 01731
01CY ATTN OPR HAROLD GARDNER
01CY ATTN LKB
KENNETH S.W. CHAMPION
01CY ATTN OPR ALVA T. STAIR
01CY ATTN PHD JURGEN BUCHAU
01CY ATTN PHD JOHN P. MULLEN

AF WEAPONS LABORATORY
KIRTLAND AFT, NM 87117
01CY ATTN SUL
01CY ATTN CA ARTHUR H. GUENTHER
01CY ATTN NTYCE 1LT. G. KRAJEI

AFTAC
PATRICK AFB, FL 32925
01CY ATTN TN

AIR FORCE AVIONICS LABORATORY
WRIGHT-PATTERSON AFB, OH 45433
01CY ATTN AAD WADE HUNT
01CY ATTN AAD ALLEN JOHNSON

DEPUTY CHIEF OF STAFF
RESEARCH, DEVELOPMENT, & ACQ
DEPARTMENT OF THE AIR FORCE
WASHINGTON, D.C. 20330
01CY ATTN AFRDQ

HEADQUARTERS
ELECTRONIC SYSTEMS DIVISION
DEPARTMENT OF THE AIR FORCE
HANSCOM AFB, MA 01731
01CY ATTN J. DEAS

HEADQUARTERS
ELECTRONIC SYSTEMS DIVISION/YSEA
DEPARTMENT OF THE AIR FORCE
HANSCOM AFB, MA 01732
01CY ATTN YSEA

HEADQUARTERS
ELECTRONIC SYSTEMS DIVISION/DC
DEPARTMENT OF THE AIR FORCE
HANSCOM AFB, MA 01731
01CY ATTN DCKC MAJ J.C. CLARK

COMMANDER
FOREIGN TECHNOLOGY DIVISION, AFSC
WRIGHT-PATTERSON AFB, OH 45433
01CY ATTN NICD LIBRARY
01CY ATTN ETDP B. BALLARD

COMMANDER
ROME AIR DEVELOPMENT CENTER, AFSC
GRIFFISS AFB, NY 13441
01CY ATTN DOC LIBRARY/TSLD
01CY ATTN OCSE V. COYNE

SAMSO/SZ
POST OFFICE BOX 92960
WORLDWAY POSTAL CENTER
LOS ANGELES, CA 90009
(SPACE DEFENSE SYSTEMS)
01CY ATTN SZJ

STRATEGIC AIR COMMAND/XPFS
OFFUTT AFB, NB 68113
01CY ATTN ADWATE MAJ BRUCE BAUER
01CY ATTN NRT
01CY ATTN DOK CHIEF SCIENTIST

SAMSO/SK
P.O. BOX 92960
WORLDWAY POSTAL CENTER
LOS ANGELES, CA 90009
01CY ATTN SKA (SPACE COMM SYSTEMS)
M. CLAVIN

SAMSO/MN
NORTON AFB, CA 92409
(MINUTEMAN)
01CY ATTN MNNL

COMMANDER
ROME AIR DEVELOPMENT CENTER, AFSC
HANSCOM AFB, MA 01731
01CY ATTN EEP A. LORENTZEN

DEPARTMENT OF ENERGY
LIBRARY ROOM G-042
WASHINGTON, D.C. 20545
01CY ATTN DOC CON FOR A. LABOWITZ

DEPARTMENT OF ENERGY
ALBUQUERQUE OPERATIONS OFFICE
P.O. BOX 5400
ALBUQUERQUE, NM 87115
01CY ATTN DOC CON FOR D. SHERWOOD

EG&G, INC.
LOS ALAMOS DIVISION
P.O. BOX 809
LOS ALAMOS, NM 85544
01CY ATTN DOC CON FOR J. BREEDLOVE

UNIVERSITY OF CALIFORNIA
LAWRENCE LIVERMORE LABORATORY
P.O. BOX 808
LIVERMORE, CA 94550
01CY ATTN DOC CON FOR TECH INFO DEPT
01CY ATTN DOC CON FOR L-389 R. OTT
01CY ATTN DOC CON FOR L-31 R. HAGER

LOS ALAMOS NATIONAL LABORATORY
P.O. BOX 1663
LOS ALAMOS, NM 87545
01CY ATTN DOC CON FOR J. WOLCOTT
01CY ATTN DOC CON FOR R.F. TASCHEK
01CY ATTN DOC CON FOR E. JONES
01CY ATTN DOC CON FOR J. MALIK
01CY ATTN DOC CON FOR R. JEFFRIES
01CY ATTN DOC CON FOR J. ZINN
01CY ATTN DOC CON FOR P. KEATON
01CY ATTN DOC CON FOR D. WESTERVELT
01CY ATTN D. SAPPENFIELD

SANDIA LABORATORIES
P.O. BOX 5800
ALBUQUERQUE, NM 87115
01CY ATTN DOC CON FOR W. BROWN
01CY ATTN DOC CON FOR A. THORNBROUGH
01CY ATTN DOC CON FOR T. WRIGHT
01CY ATTN DOC CON FOR D. DAHLGREN
01CY ATTN DOC CON FOR 3141
01CY ATTN DOC CON FOR SPACE PROJECT DIV

SANDIA LABORATORIES
LIVERMORE LABORATORY
P.O. BOX 969
LIVERMORE, CA 94550
01CY ATTN DOC CON FOR B. MURPHEY
01CY ATTN DOC CON FOR T. COOK

OFFICE OF MILITARY APPLICATION
DEPARTMENT OF ENERGY
WASHINGTON, D.C. 20545
01CY ATTN DOC CON DR. YO SONG

OTHER GOVERNMENT

INSTITUTE FOR TELECOM SCIENCES
NATIONAL TELECOMMUNICATIONS & INFO ADMIN
BOULDER, CO 80303
01CY ATTN A. JEAN (UNCLASS ONLY)
01CY ATTN W. UTLAUT
01CY ATTN D. CROMBIE
01CY ATTN L. BERRY

NATIONAL OCEANIC & ATMOSPHERIC ADMIN
ENVIRONMENTAL RESEARCH LABORATORIES
DEPARTMENT OF COMMERCE
BOULDER, CO 80302
01CY ATTN R. GRUBB
01CY ATTN AERONOMY LAB G. REID

DEPARTMENT OF DEFENSE CONTRACTORS

AEROSPACE CORPORATION
P.O. BOX 92957
LOS ANGELES, CA 90009
01CY ATTN I. GARFUNKEL
01CY ATTN T. SALMI
01CY ATTN V. JOSEPHSON
01CY ATTN S. BOWER
01CY ATTN D. OLSEN

ANALYTICAL SYSTEMS ENGINEERING CORP
5 OLD CONCORD ROAD
BURLINGTON, MA 01803
01CY ATTN RADIO SCIENCES

AUSTIN RESEARCH ASSOC., INC.
1901 RUTLAND DRIVE
AUSTIN, TX 78758
01CY ATTN L. SLOAN
01CY ATTN R. THOMPSON

BERKELEY RESEARCH ASSOCIATES, INC.
P.O. BOX 983
BERKELEY, CA 94701
01CY ATTN J. WORKMAN
01CY ATTN C. PRETTIE
01CY ATTN S. BRECHT

BOEING COMPANY, THE
P.O. BOX 3707
SEATTLE, WA 98124
01CY ATTN G. KEISTER
01CY ATTN D. MURRAY
01CY ATTN G. HALL
01CY ATTN J. KENNEY

CHARLES STARK DRAPER LABORATORY, INC.
555 TECHNOLOGY SQUARE
CAMBRIDGE, MA 02139
01CY ATTN D.B. COX
01CY ATTN J.P. GILMORE

COMSAT LABORATORIES
LINTHICUM ROAD
CLARKSBURG, MD 20734
01CY ATTN G. HYDE

CORNELL UNIVERSITY
DEPARTMENT OF ELECTRICAL ENGINEERING
ITHACA, NY 14850
01CY ATTN D.T. FARLEY, JR.

ELECTROSPACE SYSTEMS, INC.
BOX 1359
RICHARDSON, TX 75080
01CY ATTN H. LOGSTON
01CY ATTN SECURITY (PAUL PHILLIPS)

EOS TECHNOLOGIES, INC.
606 Wilshire Blvd.
Santa Monica, Calif 90401
01CY ATTN C.B. GABBARD
01CY ATTN R. LELEVIER

ESL, INC.
495 JAVA DRIVE
SUNNYVALE, CA 94086
01CY ATTN J. ROBERTS
01CY ATTN JAMES MARSHALL

GENERAL ELECTRIC COMPANY
SPACE DIVISION
VALLEY FORGE SPACE CENTER
GODDARD BLVD KING OF PRUSSIA
P.O. BOX 8555
PHILADELPHIA, PA 19101
01CY ATTN M.H. BORTNER
SPACE SCI LAB

GENERAL ELECTRIC COMPANY
P.O. BOX 1122
SYRACUSE, NY 13201
01CY ATTN F. REIBERT

GENERAL ELECTRIC TECH SERVICES
CO., INC.
HMES
COURT STREET
SYRACUSE, NY 13201
01CY ATTN G. MILLMAN

EOPHYSICAL INSTITUTE
NIVERSITY OF ALASKA
AIRBANKS, AK 99701
(ALL CLASS ATTN: SECURITY OFFICER)
01CY ATTN T.N. DAVIS (UNCLASS ONLY)
01CY ATTN TECHNICAL LIBRARY
01CY ATTN NEAL BROWN (UNCLASS ONLY)

TE SYLVANIA, INC.
LECTRONICS SYSTEMS GRP-EASTERN DIV
7 A STREET
IEEDHAM, MA 02194
01CY ATTN DICK STEINHOF

ISS, INC.
! ALFRED CIRCLE
3EDFORD, MA 01730
01CY ATTN DONALD HANSEN

ILLINOIS, UNIVERSITY OF
107 COBLE HALL
150 DAVENPORT HOUSE
CHAMPAIGN, IL 61820
(ALL CORRES ATTN DAN MCCLELLAND)
01CY ATTN K. YEH

INSTITUTE FOR DEFENSE ANALYSES
1801 NO. BEAUREGARD STREET
ALEXANDRIA, VA 22311
01CY ATTN J.M. AEIN
01CY ATTN ERNEST BAUER
01CY ATTN HANS WOLFARD
01CY ATTN JOEL BENGSTON

INTL TEL & TELEGRAPH CORPORATION
500 WASHINGTON AVENUE
NUTLEY, NJ 07110
01CY ATTN TECHNICAL LIBRARY

JAYCOR
11011 TORREYANA ROAD
P.O. BOX 85154
SAN DIEGO, CA 92138
01CY ATTN J.L. SPERLING

JOHNS HOPKINS UNIVERSITY
APPLIED PHYSICS LABORATORY
JOHNS HOPKINS ROAD
LAUREL, MD 20810
01CY ATTN DOCUMENT LIBRARIAN
01CY ATTN THOMAS POTEMRA
01CY ATTN JOHN DASSOULAS

KAMAN SCIENCES CORP
P.O. BOX 7463
COLORADO SPRINGS, CO 80933
01CY ATTN T. MEAGHER

KAMAN TEMPO-CENTER FOR ADVANCED STUDIES
816 STATE STREET (P.O DRAWER QQ)
SANTA BARBARA, CA 93102
01CY ATTN DASIAC
01CY ATTN WARREN S. KNAPP
01CY ATTN WILLIAM MCNAMARA
01CY ATTN B. GAMBILL

LINKABIT CORP
10453 ROSELLE
SAN DIEGO, CA 92121
01CY ATTN IRWIN JACOBS

LOCKHEED MISSILES & SPACE CO., INC
P.O. BOX 504
SUNNYVALE, CA 94088
01CY ATTN DEPT 60-12
01CY ATTN D.R. CHURCHILL

LOCKHEED MISSILES & SPACE CO., INC.
3251 HANOVER STREET
PALO ALTO, CA 94304
01CY ATTN MARTIN WALT DEPT 52-12
01CY ATTN W.L. IMHOF DEPT 52-12
01CY ATTN RICHARD G. JOHNSON DEPT 52-12
01CY ATTN J.B. CLADIS DEPT 52-12

MARTIN MARIETTA CORP
ORLANDO DIVISION
P.O. BOX 5837
ORLANDO, FL 32805
01CY ATTN R. HEFFNER

M.I.T. LINCOLN LABORATORY
P.O. BOX 73
LEXINGTON, MA 02173
01CY ATTN DAVID M. TOWLE
01CY ATTN L. LOUGHLIN
01CY ATTN D. CLARK

ONNEL DOUGLAS CORPORATION
)1 BOLSA AVENUE
ITINGTON BEACH, CA 92647
)1CY ATTN N. HARRIS
)1CY ATTN J. MOULE
)1CY ATTN GEORGE MROZ
)1CY ATTN W. OLSON
)1CY ATTN R.W. HALPRIN
)1CY ATTN TECHNICAL
LIBRARY SERVICES

SSION RESEARCH CORPORATION
5 STATE STREET
NTA BARBARA, CA 93101
01CY ATTN P. FISCHER
01CY ATTN W.F. CREVIER
01CY ATTN STEVEN L. GUTSCHE
01CY ATTN R. BOGUSCH
01CY ATTN R. HENDRICK
01CY ATTN RALPH KILB
01CY ATTN DAVE SOWLE
01CY ATTN F. FAJEN
01CY ATTN M. SCHEIBE
01CY ATTN CONRAD L. LONGMIRE
01CY ATTN B. WHITE
01CY ATTN R. STAGAT

SSION RESEARCH CORP.
'20 RANDOLPH ROAD, S.E.
.BUQUERQUE, NEW MEXICO 87106
01CY R. STELLINGWERF
01CY M. ALME
01CY L. WRIGHT

ITRE CORPORATION, THE
.O. BOX 208
EDFORD, MA 01730
01CY ATTN JOHN MORGANSTERN
01CY ATTN G. HARDING
01CY ATTN C.E. CALLAHAN

ITRE CORP
ESTGATE RESEARCH PARK
320 DOLLY MADISON BLVD
CLEAN, VA 22101
01CY ATTN W. HALL
01CY ATTN W. FOSTER

ACIFIC-SIERRA RESEARCH CORP
2340 SANTA MONICA BLVD.
OS ANGELES, CA 90025
01CY ATTN E.C. FIELD, JR.

PENNSYLVANIA STATE UNIVERSITY
IONOSPHERE RESEARCH LAB
318 ELECTRICAL ENGINEERING EAST
UNIVERSITY PARK, PA 16802
(NO CLASS TO THIS ADDRESS)
01CY ATTN IONOSPHERIC RESEARCH LAB

PHOTOMETRICS, INC.
4 ARROW DRIVE
WOBURN, MA 01801
01CY ATTN IRVING L. KOFSKY

PHYSICAL DYNAMICS, INC.
P.O. BOX 3027
BELLEVUE, WA 98009
01CY ATTN E.J. FREMOUW

PHYSICAL DYNAMICS, INC.
P.O. BOX 10367
OAKLAND, CA 94610
ATTN A. THOMSON

R & D ASSOCIATES
P.O. BOX 9695
MARINA DEL REY, CA 90291
01CY ATTN FORREST GILMORE
01CY ATTN WILLIAM B. WRIGHT, JR.
01CY ATTN WILLIAM J. KARZAS
01CY ATTN H. ORY
01CY ATTN C. MACDONALD
01CY ATTN R. TURCO
01CY ATTN L. DeRAND
01CY ATTN W. TSAI

RAND CORPORATION, THE
1700 MAIN STREET
SANTA MONICA, CA 90406
01CY ATTN CULLEN CRAIN
01CY ATTN ED BEDROZIAN

RAYTHEON CO.
528 BOSTON POST ROAD
SUDBURY, MA 01776
01CY ATTN BARBARA ADAMS

RIVERSIDE RESEARCH INSTITUTE
330 WEST 42nd STREET
NEW YORK, NY 10036
01CY ATTN VINCE TRAPANI

SCIENCE APPLICATIONS, INC.
1150 PROSPECT PLAZA
LA JOLLA, CA 92037
01CY ATTN LEWIS M. LINSON
01CY ATTN DANIEL A. HAMLIN
01CY ATTN E. FRIEMAN
01CY ATTN E.A. STRAKER
01CY ATTN CURTIS A. SMITH

SCIENCE APPLICATIONS, INC
1710 GOODRIDGE DR.
MCLEAN, VA 22102
01CY J. COCKAYNE
01CY E. HYMAN

SRI INTERNATIONAL
333 RAVENSWOOD AVENUE
MENLO PARK, CA 94025
01CY ATTN J. CASPER
01CY ATTN DONALD NEILSON
01CY ATTN ALAN BURNS
01CY ATTN G. SMITH
01CY ATTN R. TSUNODA
01CY ATTN DAVID A. JOHNSON
01CY ATTN WALTER G. CHESNUT
01CY ATTN CHARLES L. RINO
01CY ATTN WALTER JAYE
01CY ATTN J. VICKREY
01CY ATTN RAY L. LEADABRAND
01CY ATTN G. CARPENTER
01CY ATTN G. PRICE
01CY ATTN R. LIVINGSTON
01CY ATTN V. GONZALES
01CY ATTN D. MCDANIEL

TECHNOLOGY INTERNATIONAL CORP
75 WIGGINS AVENUE
BEDFORD, MA 01730
01CY ATTN W.P. BOQUIST

TOYON RESEARCH CO.
P.O. Box 6890
SANTA BARBARA, CA 93111
01CY ATTN JOHN ISE, JR.
01CY ATTN JOEL GARBARINO

TRW DEFENSE & SPACE SYS GROUP
ONE SPACE PARK
REDONDO BEACH, CA 90278
01CY ATTN R. K. PLEBUCH
01CY ATTN S. ALTSCHULER
01CY ATTN D. DEE
01CY ATTN D/ STOCKWELL
SNTF/1575

VISIDYNE
SOUTH BEDFORD STREET
BURLINGTON, MASS 01803
01CY ATTN W. REIDY
01CY ATTN J. CARPENTER
01CY ATTN C. HUMPHREY

UNIVERSITY OF PITTSBURGH
PITTSBURGH, PA 15213
01CY ATTN: N. ZABUSKY

DIRECTOR OF RESEARCH
U.S. NAVAL ACADEMY
ANNAPOLIS, MD 21402
02CY

DEPARTMENT OF THE NAVY

NAVAL RESEARCH LABORATORY
Washington, D.C. 20375-5000

OFFICIAL BUSINESS
PENALTY FOR PRIVATE USE, $300

POSTAGE AND FEES PAID
DEPARTMENT OF THE NAVY
DoD-316
THIRD CLASS MAIL

END

FILMED

8-85

DTIC